RADARSAT SAR Data for Landuse/Land-Cover Classification in the Rural-Urban Fringe of the Greater Toronto Area

Yifang Ban
Professor, Royal Institute of Technology
Stockholm, Sweden
Yifang@infra.kth.se

Qiaojun Wu
Graduate Student, York University
Toronto, Canada
qiaojun@yorku.ca

SUMMARY

This research investigates the capability of the multitemporal RADARSAT Fine-Beam C-HH SAR imagery for extracting landuse/land-cover information in the rural-urban fringe of the Greater Toronto Area (GTA) using various image processing techniques and classification algorithms. Five-date RADARSAT fine-beam SAR images were acquired during May to August in 2002. The major landuse/land-cover classes were high-density built-up areas, low-density built-up areas, roads, forests, parks, golf courses, water and three types of agricultural lands. These ten classes were chosen to characterize the complex landuse/land-cover types in the rural-urban fringe of the GTA. The results demonstrated that, for identifying landuse/land-cover classes, five-date raw SAR imagery yielded very poor result due to speckles. The best result was achieved for combined Mean, Standard Deviation and Correlation texture images using artificial neural networks (ANN) (overall accuracy: 89.7% and Kappa: 0.886). These high accuracies indicated that RADARSAT fine-beam SAR has the potential for operational landuse/land-cover mapping in urban environments.

KEYWORDS: *Multitemporal, RADARSAT SAR, Landuse/Land-cover, Classification*

INTRODUCTION

Information on landuse/land-cover is an important element in forming policies regarding economic, demographic, and environmental issues at national, regional and global levels. The Greater Toronto Area (GTA), like many other urban areas in the world, is undergoing rapid expansion and sprawling. The rural-urban fringe of the GTA is among the most rapidly changing elements in the landscape. Mapping landuse/land-cover of the rural-urban fringe in a timely and accurate manner is thus of great importance for urban planning, landuse planning, conservation of biodiversity and sustainable management of land resources.

With its all-weathered capability, SAR instruments have been receiving considerable attention in the remote sensing community. Very few studies, however, were focused on urban applications of radar data in comparison to other aspects of SAR research and application due to the diversity of natural and artificial elements in urban landscapes, the lack of high-resolution satellite SAR data, and the lack of effective methodology to extract information from SAR data (e.g., Henderson and Xia, 1997 & 1998; Weydhal, 2002; Dell'Acqua and Gamba, 2003). Although several studies have been done on SAR imagery over the urban areas, they all dealt with very few classes. For examples, Strozzi et al. (2000) adopted a classification scheme of four classes, namely urban areas, water, forest and sparse vegetation in a landuse mapping project in three test sites in Europe with ERS SAR interferometry. Grey and Luckman (2003) mapped urban extent using ERS SAR interferometric images of South Wales, United

Kingdom. Their work, however, used only two classes—urban and non-urban areas. Thus, there is a strong need to evaluate the capability of RADARSAT fine-beam SAR data for land cover mapping in rural-urban fringe.

The objective of this research is to evaluate the capability of the multitemporal RADASAT fine-beam C-HH SAR data for extracting landuse/land-cover information in the rural-urban fringe of the GTA.

STUDY AREA AND DATA DESCRIPTION

The study area is located in the north and northwest part of the GTA, Ontario, Canada, where rapid urban expansion and sprawl has encroached onto the Oak Ridges Moraine, one of the most distinct and environmentally significant landforms in southern Ontario. The major landuse/land-cover classes were high-density built-up areas, low-density built-up areas, roads, forests, parks, golf courses, water and three types of agricultural lands (winter wheat/rye, pasture, and soybeans/corn).These ten classes, adapted from USGS landuse/land-cover classification scheme, were chosen to characterize the complex landuse/land-cover types in the rural-urban fringe of the GTA.

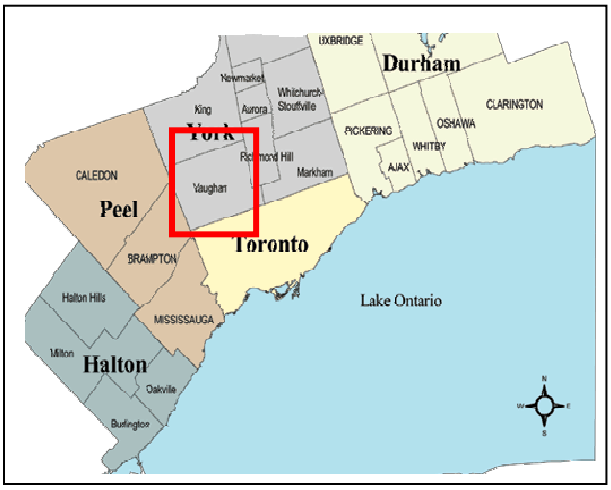

Figure 1. The Study Area: Rural-Urban Fringe of GTA, Ontario, Canada (GTMA, 2003)

Five-date RADARSAT fine-beam C-HH SAR images with a spatial resolution of 10 meters and a pixel spacing of 6.25 meter were acquired during May to August in 2002. The detailed descriptions of these images are given in Table 1.

Acquisition date	Beam position	Orbit	Incidence angle range (degree)
May 14 2002	Fine 2 Far	Ascending	39.5-42.5
Jul. 1 2002	Fine 2	Ascending	39.3-42.1
Jul. 16 2002	Fine 4 Near	Descending	43.2-45.5
Aug. 9 2002	Fine 4 Near	Descending	43.2-45.5
Aug. 18 2002	Fine 2	Ascending	39.3-42.1

Table 1 RADARSAT Fine-Beam SAR Imagery

These five-date SAR images can be grouped into two categories based on the orbit and beam position. The first group, May 14, July 1 and Aug. 18 images, were acquired in an ascending orbit with Fine-2 beam-mode, except that May 14 image was in beam-mode Fine 2 Far rather than Fine 2. The second group, July 16 and Aug 09 images were acquired with Fine 4 Near beam position in a descending orbit.

Field data on various landuse/land-cover types, their roughness and moisture conditions, vegetation heights, gound-coverages were collected during each satellite overpass. Photographs were taken during fieldwork to assist image interpretation and analysis. Other sources of data were also used to georeference SAR data and to assist selecting ground reference data for classification calibration and validation and they include:

(1) Landsat ETM+ data, 2002
(2) Orthophotos at 0.5 meter resolution, 1999
(3) National Topographic Database (NTDB) vector data
(4) DEM, 30m resolution
(5) Published maps

METHODOLOGY

Geometric Correction of SAR Images

To remove these relief displacements and bring the five images from two opposite look-directions to the same database, multi-temporal RADARSAT SAR imagery were orthorectifed to the NTDB database using satellite orbital models and a digital elevation model at 30m resolution.

Image Processing and Analysis

To reduce speckle in SAR images, three adaptive speckle filters, namely Gamma, Enhanced Lee (EL) and Enhanced Frost (EF) filters were tested in this study. These adaptive speckle filters smooth speckle in homogeneous while preserving texture and high frequency information in heterogeneous areas. Different filter sizes were also tested as they affect the quality of processed images. If the filter is too small, the noise filtering algorithm is not effective. If the filter is too large, subtle details of the image are lost in the filtering process. After preliminary trials, an 11x11 filter size was selected in this study for all three filters.

Texture is one of the significant parameters recognized by the human visual system, besides pixel brightness and color, for identifying objects or regions of interest in an image. Various studies showed that in most cases (if not all), texture, not intensity, is the most important source of information in high-resolution radar images (e.g., Ulaby et al., 1986; Dobson et al., 1995; Dell'Acqua, and Gamba , 2003). In this study, GLCM-based texture measures including Mean, Standard Deviation (SD), Correlation and Entropy were analyzed using PCI Geomatica. Using second-order spatial statistics, GLCM is a two-dimensional array that can provide conditional joint probabilities of all pair-wise combinations of pixels within a computation window. An 11x11 window size was selected based on trials and in order to be comparable with filtered images.

Selection of Calibration and Validation Blocks

For each landuse/land-cover class, pixel sample blocks were randomly extracted in order to calibrate the maximum-likelihood classifier and to train the artificial neural network. To assess the accuracy of the classifications, validation pixels, independent from the calibration pixels, were randomly selected for each landuse/land-cover class. The selections of calibration and validation blocks were based on field data, Landsat ETM+ images, NTDB vectors and maps. In this study, more than 1000 pixels are randomly selected throughout the image as ground reference data for each of the 10 landuse/land-cover classes. Among them, 200 pixels were used for validation of the classification accuracies while the rest were used as training data to calibrate classifiers.

Image Classification

To evaluate the effectiveness of different image processing techniques for extraction of landuse/land-cover information, it is necessary to classify the raw SAR images, filtered images and texture images. Maximum Likelihood Classifier (MLC), a widely used statistical classifier, was first performed as a basis for comparison between different image processing techniques.

Artificial neural network (ANN) classifiers are computer programs designed to simulate human learning process through establishment and reinforcement of linkages between input data and output data. ANN presents a non-parametric, distribution-free approach to image classification. ANN classifiers have been applied to multi-source, multi-dimension data to overcome the limits of classical classifiers such as MLC, which is based on some untenable assumptions about the dataset such as the normal distribution of the data. Several researchers have found ANN to be a more robust classifier than the traditional statistical approaches (e.g., Benediktsson et al., 1990, Ban, 2003). In this study, a multilayer feed-forward neural network classifier in PCI Geomatica was tested to compare with MLC.

Post-Classification Filtering

Post-classification processing can improve classification results considerably. Isolated pixels with other class assignment within a large homogenous area can be removed and mixed pixels at the border between classes can be assigned to the dominant class using simple filters. In this study, Mode filter was applied to classification results.

Classification Accuracy Assessment

To assess the quality of the image classifications, various measures including overall accuracy and Kappa coefficient of agreement (or Kappa) were analyzed to compare classification results with the validation or reference data in confusion matrices. Overall accuracy is the total number of correctly classified samples (diagonal cells in a confusion matrix) divided by the total number of reference pixels. Utilizing all elements from the confusion matrix, Kappa coefficient is a measure of the difference between the actual agreement between reference data and a classification and the change agreement between the reference data and a classification (Lillesand & Kiefer 2000). Kappa takes into account both errors of commission and omission, and thus provides a more complete picture of the information comprising the confusion matrix than overall accuracy (Jensen, 2004).

RESULTS AND DISCUSSION

Geometric Correction

The five SAR images were ortho-rectified into the NTDB/ETM+ database using a 30m DEM and 70 ground control points. The RMSs for both x and y directions were less than 1.4 pixels (pixel spacing is 6.25m).

Classifications of Raw SAR Images

The results demonstrated that, for identifying landuse/land-cover classes, single-date raw SAR data yielded very poor results using MLC (Table 2). The combination of five-date SAR presented an 11% improvement of classification accuracy over the best single-date classification. The overall validation accuracy and kappa, however, were very low (overall accuracy: 37.25% and kappa: 0.3). The poor accuracies may be, in part, because MLC is not an effective classifier for classification of SAR data classifications due to speckle in the raw radar images.

ANN classification method performed slightly better than MLC for individual SAR images and for five-date combination. The classification accuracy for all images increased slightly except that of August 9 image which decreased slightly (0.2%). The results indicated that ANN was likely affected by speckles in the raw SAR images and therefore raw SAR images were not useful for extraction of landuse/land-cover information.

Classifications of Filtered SAR Images

Enhanced Frost, Gamma and Enhanced Lee Filters significantly improved the classification accuracies (Table 2). Classification accuracies for five-date SAR filtered images achieved over 70% while kappa is over 0.65. This represents more than 30% improvement over the five-date raw SAR data and more than 0.5 for kappa. Combining any two or three sets of them, however, decreased the accuracies due to the confusion caused by mixing up similar information content in these three sets of filtered images.

ANN Classifications of filtered SAR images improved classification accuracies 4-6% compared to MLC. Classification of combined filtered images with ANN, however, yielded much better results than that of MLC. The overall accuracies for combined EL and Gamma filtered images, combined EF and Gamma filtered images, combined EF and EL filtered images, and combination of all filtered images were 79.5%, 77.55%, 75.05 and 80.4% respectively which represent 21%, 21.8%, 17.6% and 33.95% improvement over their respective counterparts with MLC. It clearly demonstrates that ANN is more robust than MLC as ANN can minimize confliction of similar signatures between images while extracting useful information from them.

Processing Technique	**MLC Accuracy**				**ANN Accuracy**			
			Mode filter				**Mode filter**	
	overall %	kappa	overall%	kappa	Overall%	kappa	Overall%	kappa
May 14	23.75	0.153	26.4	0.182	24.6	0.180	29.55	0.234
July 01	25.95	0.177	29.1	0.212	26.15	0.188	30.6	0.237
July 16	20.85	0.121	22.3	0.137	22.25	0.155	26.3	0.199
Aug 09	24.6	0.162	28.85	0.209	24.40	0.187	31.05	0.259
Aug 18	25.7	0.174	27.75	0.197	25.95	0.204	29.6	0.243
Five-date Raw SAR	37.25	0.303	45.95	0.399	39.85	0.332	47.45	0.416
EL	70.0	0.667	77.0	0.744	74.2	0.713	79.15	0.768
Gamma	69.15	0.657	75.85	0.732	74.9	0.721	82.3	0.803
EF	71.75	0.686	75.85	0.732	78.25	0.758	81.15	0.791
EL+Gamma	58.5	0.539	64.3	0.603	79.5	0.772	87.75	0.864
EF+Gamma	55.75	0.508	57.6	0.529	77.55	0.751	81.35	0.793
EF+EL	57.45	0.527	61.4	0.571	75.05	0.723	76.6	0.740
EL+EF+Gamma	46.45	0.405	47.65	0.418	80.4	0.782	84.85	0.832
Mean	74.95	0.722	75.7	0.730	82.65	0.807	83.5	0.817
SD	62.65	0.585	64.7	0.608	65.5	0.617	67.3	0.637
Entropy	52.65	0.474	53.95	0.488	54.0	0.489	54.95	0.499
Correlation	31.55	0.239	32.95	0.255	30.3	0.226	31.0	0.233
Mean + SD	85.25	0.836	86.2	0.847	88.45	0.872	88.8	0.876
Mean + Correlation	83.55	0.814	84.05	0.821	86.55	0.851	87.3	0.859
Mean+SD+Entropy	88.2	0.869	89.7	0.886	87.9	0.866	89.05	0.878
Mean+SD+correlation	88.55	0.873	89.45	0.883	89.7	0.886	90.25	0.892
Mean + EF	82.1	0.801	84.4	0.827	83.0	0.811	84.05	0.823
Mean + SD + EF	84.25	0.825	85.8	0.842	86.25	0.847	87.5	0.861

Table 2 Comparison of MLC and ANN Classifiers for Selected Images

Classifications of Texture Images

For texture measures, Mean texture performed better than other measures using MLC (Table 2). five-date Mean images produced the best result among all single-set data using MLC. Combinations of various texture measures, which can extract unique spatial relationships from the same SAR data, showed improvement over single-set texture measure because of their different, complementary information. The best result using MLC was achieved with combined Mean, Standard Deviation and Correlation texture images (overall: 88.55% and kappa 0.873). This represents over 50% increase in the classification accuracy over that of the five-date raw SAR images.

Similar to MLC, Mean texture performed better than other measures using ANN. ANN classification of the Mean texture achieved over 82% accuracy (kappa: 0.8) and this represents almost 8% improved over MLC. As for combined texture images, four combinations were evaluated using ANN (Table 2). Among these four combinations, all accuracies improved slightly except the accuracy of combined Mean, SD and Entropy images with a 0.3% decrease. The best classification result of 89.7% (kappa, 0.886) was achieved with combined Mean, SD and Correlation images, which represents a 1.15% increase over the same datasets with MLC classifier. These results indicate that the performances of MLC and ANN are similar for texture images. MLC is a fast, easy method for operational use while ANN is relatively complex and time-consuming.

Table 3 shows that almost all landuse/land-cover classes achieved excellent accuracies except Golf courses which is confused with parks and water due to their similar backscatter. The results indicate that RADARSAT fine-beam SAR data has the potential for operational landuse/land-cover mapping in urban environments.

	Reference Data											
Classified Data	Water	Roads	LB	HB	Golf courses	Forest	Parks	W. Wheat/rye	Pasture	Soybeans/corn	Total	**User's Accuracy (%)**
Water	187	0	0	0	24	0	0	0	0	0	211	89
Roads	3	169	0	0	1	0	6	0	0	10	189	89
LB	0	4	194	6	0	16	0	0	0	2	222	87
HB	0	0	0	193	0	0	0	0	0	0	193	100
Golf courses	10	3	0	0	148	0	14	0	0	0	175	85
Forest	0	6	6	1	0	183	0	0	1	3	200	92
Parks	0	7	0	0	27	0	178	0	0	0	212	84
W. Wheat/rye	0	10	0	0	0	1	0	181	23	0	215	84
Pasture	0	0	0	0	0	0	0	19	176	0	195	90
Soybeans/corn	0	1	0	0	0	0	2	0	0	185	188	98
Total	200	200	200	200	200	200	200	200	200	200	2000	
Producer's Accuracy (%)	94	85	97	97	74	92	89	91	88	93		

Table 3. Confusion Matrix for Combined 'Mean', 'SD' and 'Correlation' Texture Images Using ANN

Post-Classification Filtering

The results also showed that the overall accuracies and kappa coefficients for almost all classifications improved using a 3 X 3 mode filter to clean up the isolated class pixels (Table 2).

CONCLUSION

Multitemporal RADARSAT Fine-Beam SAR data were evaluated for extracting landuse/land-cover information in the rural-urban fringe of the Greater Toronto Area (GTA). Five-date RADARSAT fine-beam SAR images were acquired during May to August in 2002. The major landuse/land-cover classes were high-density built-up areas, low-density built-up areas, roads, forests, parks, golf courses, water and three types of agricultural lands. Various SAR image processing techniques and classification algorithms were tested in this research. The results demonstrated that, for identifying landuse/land-cover classes using either MLC or ANN, both single-date and five-date raw SAR images yielded very poor result due to speckles in the raw images. Enhanced Frost, Gamma and Enhanced Lee Filters significantly improved the classification accuracies by more than 31%. Texture measures proved to be superior over filtered images. Five-date Mean images produced the best result among the texture measures examined. Combinations of various texture measures showed improvement over single-set texture measure because of their different, complementary information. The best result using MLC was achieved with combined Mean, Standard Deviation and Correlation texture images (Overall accuracy: 88.55%, Kappa: 0.873). This represents over 50% increase in the classification accuracy over that of the five-date raw SAR images. Similar to MLC, the best ANN result was achieved using combined Mean, Standard Deviation and Correlation texture images (Overall accuracy: 89.7%, Kappa: 0.886). These high accuracies indicated that RADARSAT fine-beam SAR has the potential for operational landuse/land-cover mapping in urban environments.

As for the comparison of classifiers, most of the classifications tested using ANN showed only slight improvements over those with MLC except significant improvements observed for combined filtered images. These results indicate that the performances of MLC and ANN are rather similar for landuse/land-cover classifications in the rural-urban fringe using RADARSAT fine-beam SAR data.

ACKNOWLEDGEMENT

Financial support for this project was provided through a Natural Sciences and Engineering Research Council of Canada (NSERC) Research Grant awarded to Dr. Yifang Ban. The RADARSAT fine-beam SAR images were provided by the Canadian Space Agency to Dr. Yifang Ban through RADARSAT-1 Data for Research Use Program.

BIBLIOGRAPHY

Ban, Y., 2003. Synergy of multitemporal ERS-1 SAR and landsat TM data for classification of agricultural crops. Canadian Journal of Remote Sensing. Vol. 29, No. 4, pp. 518-526.

Benediktsson, J. A., Swain, P. H., and Ersoy, O. K., 1990. Neural Network Approaches Versus Statistical Methods in Classification of Multisource Remote Sensing Data, IEEE Transactions on Geoscience and Remote Sensing, 28 (4): 540-552.

Dell'Acqua, F. and Gamba, P., 2003. Texture-based characterization of urban environments on satellite SAR images. IEEE Transactions on Geoscience and Remote Sensing, 41(1): 153-159.

Dobson, M., Ulaby, F. and Pierce, L., 1995. Land-cover classification and estimation of terrain attributes using synthetic aperture radar. Remote Sensing of Environment, 51:199–214.

Grey, W. and Luckman, A., 2003. Mapping Urban Extent Using Satellite Radar Interferometry. Photogrammetic Engineering and Remote Sensing, 69 (9): 957-962.

GTMA, 2003. Map of Greater Toronto Area, The Greater Toronto Marketing Alliance (GTMA), http://www.greater.toronto.on.ca/ataglance/mapprofile.html#toarea.

Henderson, F. M. and Xia, Z. G., 1997. SAR applications in human settlement detection, population estimation and urban land use pattern analysis: A status report, IEEE Transactions On Geoscience And Remote Sensing 35 (1): 79-85.

Henderson, F. M. and Xia, Z. G., 1998. Chapter 15: radar applications in urban analysis, settlement detection and population estimation, 3rd ed. Manual of Remote Sensing, vol. 2. Wiley, New York, 759– 761.

Jensen, J. R., 2004. Introductory digital image processing: a remote sensing perspective 3rd Ed. New York: Prentice-Hall, Inc.

Lillesand, T. M. and Kiffer, R. W., 2000. Remote sensing and image interpretation, 4th Edition. John Wiley and Sons, New York, NY.

Strozzi, T., Dammert, P. B. G., Wegmuller, U., Martinez, J.-M., Askne, J. I. H., Beaudoin, A., Hallikainen, N. T., 2000. Landuse mapping with ERS SAR interferometry. IEEE Transactions on Geoscience and Remote Sensing, 38 (2): 766–775.

Ulaby, F. T., Kouyate, F., Brisco, B., and Williams, T. H. L., 1986. Textural information in SAR images, IEEE Trans. Geosci. Remote Sensing, GE–24: 235–245.

Weydahl, D. J., 2002. Backscatter changes of urban features using multiple incidence angle RADARSAT images. Canadian Journal of Remote Sensing, 28 (6): 782-793.